

Thermomagnetism of reversible transverse susceptibility

Jyh-Shinn Yang

Division of General Education, National Taiwan Ocean University, Keelung, Taiwan, Republic of China

Ching-Ray Chang and Ivo Klik

Department of Physics, National Taiwan University, Taipei, Taiwan, Republic of China

(Received 17 October 1994)

Thermal relaxation is taken into account in analysis of the reversible transverse susceptibility (RTS) of an interacting particulate system described within the mean-field approximation. Particle orientation is given by a texture function with independent in-plane and out-of-plane components. The shape and location of the RTS peak at coercivity critically depends on temperature, texture, and on the interaction strength while the peak at the anisotropy field gradually merges with the coercivity peak at a strong-coupling field. There are only two peaks remaining in RTS measurement for either a strongly coupled or a well-aligned system. Thus, peak-detection techniques fail to distinguish the anisotropy field and coercivity.

I. INTRODUCTION

Recently it was shown that measurements of reversible transverse susceptibility yield valuable information not only about the fundamental magnetic material properties, but also about the characteristics of the magnetic recording performance.^{1,2} However, the phenomenon of reversible susceptibility (RS) is very complex and not yet fully understood, despite numerous attempts to develop a first-principles calculation of RS in ferromagnetic materials. Assuming coherent rotation of magnetic moments in single-domain particles, the magnetization curve $M(H)$ of a uniaxial crystal, with H oriented in the hard direction, has a singularity at the saturation point, i.e., when the applied field equals the anisotropy field³ H_k . For a randomly oriented system, the magnetization curve shows a smooth dependence on applied field, with no apparent vestiges of the singularity at $H = \pm H_k$. However, it has been shown that the singular point behavior becomes apparent again in the successive derivatives $d^n M/dH^n$ plotted^{3,4} as functions of H . Usually, the detection of singular behavior of reversible transverse susceptibility (RTS) is much easier than that of reversible parallel susceptibility⁴ and despite its simplicity it is versatile and capable of relatively high sensitivity.^{5,6} Therefore, a lot of effort has been devoted in the past to analysis and measurement of RTS in ferromagnetic materials.⁴⁻⁸

The method, however, does not yield the same information about magnetic anisotropy as the torsion pendulum measurements.⁶ In particular, the RTS anisotropy peak vanishes in a system with either large particles⁴ or with strong interparticle coupling.⁶ Various approaches have been evoked to account for this failure of the RTS measurements. Expressions for the RS tensor based on coherent rotation of the magnetic moments of single-domain particles⁷ predict that the RTS function χ_t of an assembly of noninteracting single-domain particles has three cusps: at the anisotropy fields $\pm H_k$ and at the coer-

civity H_c . Investigations of the effects of distribution of anisotropy field strength and of texture in a noninteracting system show that the cusps of the theoretical curves are smeared out. In particular, the cusp at H_c is suppressed while the peaks at the $\pm H_k$ remain.⁸ The discrepancy of RTS peaks between experimental and theoretical data has been attributed to unrealistic assumptions in the basic model,⁸⁻¹¹ such as neglecting thermal relaxation effects and interparticle coupling.

Both relaxation and texture effects have been reported to suppress and shift the RTS peak at coercivity in noninteracting systems,^{8,11,12} while the position and the height of the anisotropy peak are not affected at all. For an interacting binary system with high symmetry, it has recently been found that the singular part of RTS is progressively suppressed with increasing interaction strength and the authors argued that the RTS will possibly remain finite at a nucleation field corresponding to a highly ordered state.⁹ Though the argument is only qualitative, it suggests that interactions between particles must be taken into account in analysis of experimental RTS curves. Recently, a mean-field model without thermal relaxation has been proposed to investigate the influence of interactions on RTS.¹⁰ In samples with random distribution of easy axes this model results in a gradual merging, as interaction strength is increased, of the RTS peaks at coercivity and at anisotropy field.¹⁰

Here we extend the mean-field model of Ref. 10 and study the combined effects of interactions and of thermal relaxation in particulate recording media with specified texture. In Sec. II we briefly review the calculation of a hysteresis loop for a thermally relaxing bistable system and write down the corresponding expressions for the RTS function $\chi_t(H)$. In Sec. III we present sample hysteresis loops of interacting arrays and compare two different algorithms for their computation. We find that negative coupling requires at least a three-level master equation description; a two-level master equation system is only appropriate for the positive interaction strengths

to which we confine ourselves here. We also briefly discuss the relaxation dynamics of magnetization at nonzero coupling strength. Addressing finally the RTS functions we find that within a mean-field theory the RTS peaks at $\pm H_k$ are suppressed by strong coupling and that the peak at H_c is critically influenced by both the medium texture and the coupling strength; thermal effects influence the coercivity peak only. Our results therefore show that determination of anisotropy constants from RTS peak detection is only valid in weakly interacting particular media.

II. THE MODEL

In this section we present our mean-field model, summarize briefly the methods used to calculate the hysteresis loop, and define the reversible transverse susceptibility of a thermally relaxing system.

We consider an array of identical single-domain uniaxial particles whose magnetization \mathbf{M} reverses by coherent rotation. Each particle has energy $E = KV \sin^2 \theta - V \mathbf{M} \cdot \mathbf{H}_{\text{eff}}$, where V is the (activation) volume and K is the anisotropy constant. The effective magnetic field \mathbf{H}_{eff} includes both the applied field and the interaction field from other particles, θ is the angle spanned by the particle's easy axis and its magnetization \mathbf{M} , $|\mathbf{M}| = M_s$ by assumption, and M_s is the saturation magnetization. The orientation of easy axes within the array is given by a texture function with independent in-plane and out-of-plane components allowing to model a realistic medium.⁸ The texture function used here is of the form

$$f(\theta_k, \phi_k) = \frac{1}{\mathcal{N}} \exp \left[-\frac{(\pi/2 - \bar{\theta}_k)^2}{2\sigma_\theta^2} \right] \times \exp \left[-\frac{\phi_k^2}{2\sigma_\phi^2} \right], \quad (1)$$

where \mathcal{N} is a normalization constant and the easy-axis orientation is defined by the spherical coordinates θ_k and ϕ_k , $\bar{\theta}_k$ is the angle between the applied field and the projection of the easy axis onto the media plane (Fig. 1). The parameters σ_θ and σ_ϕ control the distributions in and out of the plane, respectively.

Interparticle interactions may either be taken into account via a microscopic approach^{13–15} or via the phenomenological mean-field approximation.^{16–19} The microscopic computation requires, as a rule, too much computing power and for the purposes of RTS calculation it becomes almost impracticable. We adopt therefore the mean-field approximation in which a representative particle of the array is acted upon by the field $\mathbf{H}_{\text{eff}} = \mathbf{H} + \alpha \langle \mathbf{M} \rangle$ where \mathbf{H} is the applied magnetic field, $\langle \mathbf{M} \rangle$ is the instantaneous mean magnetization of the array and α is a coupling constant. Calculations of a hysteresis loop within this model have been reported previously^{16,17} for Stoner-Wohlfarth particles²⁰ without thermal relaxation effects. However, in a thermally relaxing system interactions provide for the slow relaxation dynamics manifesting by either quasilogarithmic or stretched-exponential behavior.¹⁹ Thus, in order to study the temperature and time dependence of the magnetic properties we should take into account both interaction

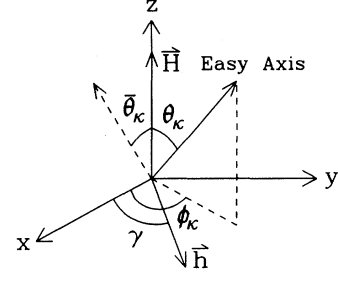


FIG. 1. Schematic diagram of a uniaxial ferromagnetic particle with main bias field \mathbf{H} and small perpendicular field \mathbf{h} . Easy-axis orientation is defined by the spherical coordinates θ_k and ϕ_k , $\bar{\theta}_k$ is the angle between the applied field and the projection of the easy axis onto the media plane, x - z plane.

and thermal relaxation effects.

In this work we treat an array of many identical particles as having two levels^{19,21} which are occupied with probabilities n_1 and $n_2 = 1 - n_1$, respectively. Its evolution is given by the master equation¹¹

$$\dot{n}_1 = -\kappa_{12}n_1 + \kappa_{21}n_2 = -\dot{n}_2, \quad (2)$$

where $\dot{n}_i = dn_i/dt$ and $\kappa_{ij} = \kappa_{i \rightarrow j} = f_0 \exp(-Q_i/k_B T)$ is the rate of thermally activated transitions from the i th to the j th level. For the prefactor we choose the value¹¹ $f_0 = e^{25}$ Hz, k_B is the Boltzman constant, T is temperature, and Q_i is the barrier height to be overcome on departure from the i th well. We shall assume that the applied field driving the hysteresis loop is in the z direction, $\mathbf{H} = [0, 0, H(t)]$, $H(t) = H_0 \cos 2\pi f t$, where f is the sweep rate and the amplitude H_0 is greater than the nucleation field H_n of the system. For $\alpha = 0$ and $\theta_k = 0$ one may set $H_0 = 2K/M_s \equiv H_n$ and the barrier heights are given by the well-known formula^{21,22} $Q_i = KV(1 \pm H/H_n)^2$. For any other alignment of the easy axis the barrier heights can only be determined numerically. If $\alpha \neq 0$ the nucleation field $H_n(\alpha)$ is not *a priori* known and in calculating the hysteresis loop we take the amplitude H_0 sufficiently large for all particles within the array to have initially only one local minimum, i.e., we solve Eq. (2) with the initial condition $n_1[H(t=0)|\theta_k, \phi_k] = 1$. There exists then no other possible metastable orientation of magnetization and $n_2[H(t=0)] = 0$. The time-dependent, nonequilibrium magnetization of an array of identical particles with easy axes in the (θ_k, ϕ_k) direction becomes¹¹

$$\begin{aligned} \mathbf{M}[H(t)|\theta_k, \phi_k] \\ = M_s \sum_{i=1}^2 n_i [\cos \phi_i \sin \theta_i, \sin \phi_i \sin \theta_i, \cos \theta_i], \end{aligned} \quad (3)$$

where (θ_i, ϕ_i) denotes the metastable orientation of magnetization, corresponding to the local minimum of the energy function, and n_i is the fraction of particles whose magnetization is in this direction. For an isolated particle $\phi_1 = \phi_k$ and $\phi_2 = \pi + \phi_k$ by symmetry, while $\theta_i = \theta_i[H(t)]$ at all times. Only if $\theta_k = 0$ does one recover the axially symmetric result $\theta_1 = 0$, $\theta_2 = \pi$,

$$\mathbf{M} = M_s [0, 0, n_1 - n_2].$$

The nonequilibrium magnetization (3) is thus expressed in terms of the four functions $\theta_i[H(t)]$ and $\phi_i[H(t)]$ which denote the instantaneous position of local energy minima and in terms of the two occupation probabilities $n_i[H(t)]$. In a noninteracting system only the occupation probabilities depend on the system's past, while the energy minima are found by simply minimizing the function $E(\theta, \phi)$ at a given field. Within the mean-field theory the mean magnetization of the system is found by averaging the magnetization (3) over the easy-axis orientations (θ_k, ϕ_k) and in this case the instantaneous position of the local minima does depend on history since each particle experiences the mean field $\mathbf{H}_{\text{eff}} = \mathbf{H} + \alpha \langle \mathbf{M} \rangle$. In implementing the mean-field approximation we proceed as follows: By virtue of our initial conditions there exists, for any easy-axis orientation, only one local energy minimum at $t=0$ and we use the easily calculated mean magnetization $\langle \mathbf{M}(0) \rangle$ to approximate the mean field an instant dt later, setting $\mathbf{H}_{\text{eff}}(t) = \mathbf{H}(t) + \alpha \langle \mathbf{M}(t-dt) \rangle$. The updated value of the mean magnetization is then used to approximate the mean field at $t=2dt$, etc. The theory is thus not entirely self-consistent since the response to the coupling field is always delayed by the integration step dt of the differential equation (2). Nonetheless, hysteresis is a memory effect, in particular where thermal relaxation is concerned,^{19,21} and the present approach is certainly preferable to the iterative procedure proposed by Atherton and Beattie^{16,17} which will be discussed in the next section.

Let now an infinitesimal perturbing field \mathbf{h} of frequency $f_h (\gg f)$ be applied perpendicular to the driving field \mathbf{H} , $\mathbf{h} = h(t)[\cos\gamma, \sin\gamma, 0]$, $h(t) = h \sin 2\pi f_p t$. The energy function acquires an additional term, $E \rightarrow E + h(t)\mathcal{E}$ where $\mathcal{E} = -VM_s \cos(\phi - \gamma) \sin\theta$. The position of the unperturbed minima is given by the equations $E_{x_\alpha} = 0$ ($E_{x_\alpha} = \partial E / \partial x_\alpha$, $x_\alpha = \theta, \phi$) and their shift δx_α due to the perturbing field is obtained by expanding these equations to the first order in h :

$$\sum_{\beta} \frac{\partial^2 E}{\partial x_\alpha \partial x_\beta} \delta x_\beta + \frac{\partial \mathcal{E}}{\partial x_\alpha} h = 0, \quad (4)$$

where the partial derivatives are to be evaluated at the unperturbed minimum. From Eq. (3) it then follows that the RTS function is given by

$$\chi_{i\xi} = M_s V h^{-1} \sum_{i=1}^2 n_i \begin{cases} \cos\phi_i \cos\theta_i \delta\theta_i \\ -\sin\phi_i \sin\theta_i \delta\phi_i, & \xi = x, \\ \sin\phi_i \cos\theta_i \delta\theta_i \\ +\cos\phi_i \sin\theta_i \delta\phi_i, & \xi = y. \end{cases} \quad (5)$$

The perturbations δn_i , calculated from Eq. (2), were shown to be negligible.¹¹

The discriminant of the linear system (4) is the Hessian of the unperturbed energy which vanishes whenever one or the other local energy minimum is annihilated (this does not necessarily hold for systems with more than two

local minima⁹). For noninteracting particles the explicit solution of Eqs. (4) and (5) was given by Aharoni *et al.*⁷ who, however, assumed that $n_1=1, n_2=0$ if $H > -H_n$, and $n_1=0, n_2=1$ if $H < -H_n$ (the Stoner-Wohlfarth model²⁰ without thermal relaxation). In reality, however, coercivity is much smaller than the nucleation field due to thermally activated magnetization reversals so that the vanishing local minimum is, as a rule,¹¹ not occupied, $\lim_{H \rightarrow -H_n} n_1 = 0$, while $\lim_{H \rightarrow -H_n} \chi_t = \infty$. Only in the Stoner-Wohlfarth model or for particles whose easy axis is perpendicular to the driving field¹¹ is the vanishing local energy minimum occupied arbitrarily close to the nucleation field. In Sec. IV we present calculations of the mean RTS function $\langle \chi_{t\xi} \rangle$ and discuss its dependence on the coupling strength, temperature, and texture.

III. HYSTERESIS PROPERTIES

In investigating the dependence of hysteresis loop on the amplitude of the driving field, most models consider only an isolated particle without thermal agitation and their results are thus only approximately applicable in the low-temperature limit to weakly interacting systems, i.e., to micronsize particles. Relaxation effects exponentially increase with the reduction of size (e.g., the ultrafine particles used in high-density magnetic recording) and thermally activated magnetization reversal currently attracts increasing attentions.^{19,23} Furthermore, interactions among the magnetic moments strongly influence the rate with which a nonequilibrium system decays towards equilibrium.¹⁹ Therefore, to understand the hysteresis properties one cannot neglect either the relaxation or the mutual interaction effects.

Dipole-dipole interactions between particles are usually treated within a microscopic approach¹³⁻¹⁵ or within the phenomenological mean-field model.¹⁶⁻¹⁹ The mean-field theory allows the simple coherent rotation model to be extended to interacting particles and provides a compromise between accuracy and convenience. Quantum mechanics has since shown that the interaction between atomic magnetic moments is due to the exchange force, but on the scale of individual particles or domains it becomes purely phenomenological.¹⁶⁻¹⁹ Within the mean-field model numerical calculations of the hysteresis loop are usually carried out iteratively, iterating from the loop of assembly of noninteracting particles.^{16,17} At applied field $\mathbf{H}(t)$ the effective field is iterated initially with $\mathbf{H}_{\text{eff}}^{(0)}(t) = \mathbf{H}(t) + \alpha \langle \mathbf{M}(t) \rangle_{\alpha=0}^{(0)}$ and then self-consistently derives the i th iteration result, the $\langle \mathbf{M}(t) \rangle_{\alpha}^{(i)}$. However, this algorithm only yields a steeper magnetization curve at coercivity for $\alpha > 0$, while the coercivity is never influenced by interaction strength since $\langle \mathbf{M}(t) \cdot \mathbf{H} \rangle_{\alpha=0} = 0$ for $H(t) = H_c$.¹⁰ Therefore, the well-known linear relationship between coercivity and packing density cannot be demonstrated.²⁴ Another possible numerical process, as described in the previous section, is $\mathbf{H}_{\text{eff}}(t) = \mathbf{H}(t) + \alpha \langle \mathbf{M}(t-dt) \rangle_{\alpha}$. Though not entirely self-consistent, it satisfies the requirement of causality and is, for small enough dt , physically more realistic. The former algorithm maintains only the history of the noninteraction system, disregarding evolution due to in-

teractions, while the latter approach keeps track of all history since saturation. It reflects the true hysteresis of the interacting system, with coercivity shifting outwards with increasing positive interaction strength (Fig. 2). We have also calculated hysteresis loops for negative coupling and found coercivity to be independent of $\alpha < 0$ since the two-level system (2) does not allow for the presence of a stable antiferromagnetic configuration. At least a three-level master equation system is required for $\alpha < 0$ and coercivity then shifts inwards with increasing coupling strength.²⁵

Using the proposed algorithm we have also calculated magnetization relaxation in an ensemble with randomly distributed easy axes at constant field. In an initially saturated system, in the absence of applied field, all particles experience only the interaction field, $\alpha \langle \mathbf{M} \rangle$ and Fig. 3 shows the resultant slowing down of the relaxation dynamics.¹⁹ For $\alpha > 0$ the relaxation is initially very slow but faster later on as the mean magnetization decays and the interaction field decreases. Relaxation is thus slower than expected from a simple exponential model, while for $\alpha < 0$ (described here within the two-level formalism) the decay is accelerated²⁶ (Fig. 3). In a perfectly aligned system of $\theta_k = 0^\circ$, in zero applied field, the equilibrium magnetization $M(\infty)$ satisfies the equation²⁷

$$\frac{M(\infty)}{M_S} = \tanh \left[2\varepsilon \frac{KV}{k_B T} \frac{M(\infty)}{M_S} \right],$$

where $\varepsilon = \alpha M_s / H_k$, which has only the trivial solution $M(\infty) = 0$ if $\varepsilon \leq k_B T / 2KV$. Parasitic nontrivial solutions appear for larger α and the mean-field theory loses consistency.

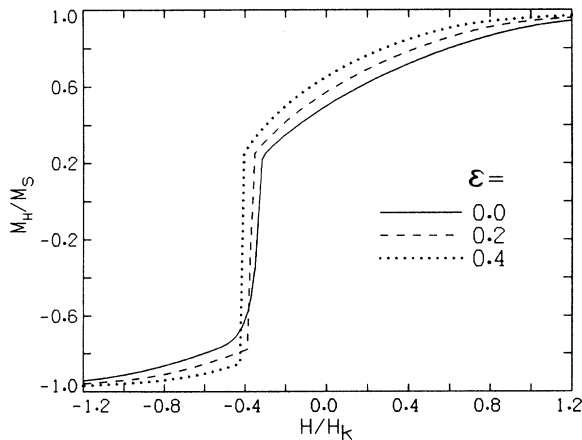


FIG. 2. Hysteresis curves for the mean-field Stoner-Wohlfarth model with uniformly distributed easy axes. Memory of the interacting effects can only be demonstrated with the newly proposed algorithm. Here $\varepsilon = \alpha M_s / H_k$, $f = 0.1$, and $KV/k_B T = 100$.

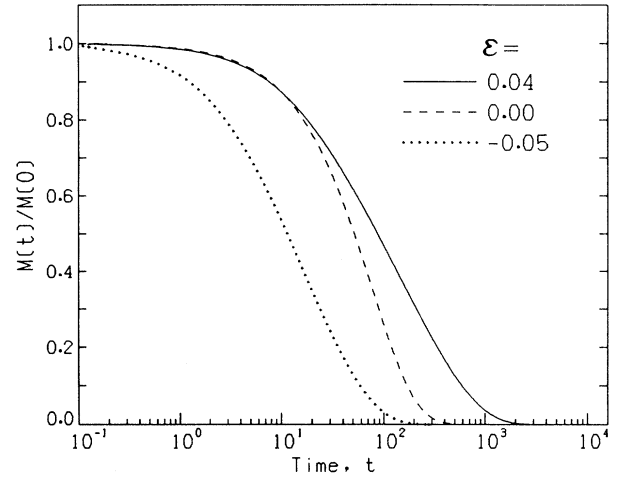


FIG. 3. Slow relaxation of a particle assembly with randomly distributed easy axes. Here $f = 0.1$ and $KV/k_B T = 30.0$.

IV. REVERSIBLE TRANSVERSE SUSCEPTIBILITY

For a Stoner-Wohlfarth particle without thermal agitation it has been shown that RTS is given by the expression^{7,10}

$$\frac{\chi_t}{\chi_0} = \frac{3}{2} \left[\cos^2 \phi_k \frac{\cos^2 \theta_M}{h_{\text{eff}} \cos \theta_M + \cos 2(\theta_M - \theta_k)} + \sin^2 \phi_k \frac{\sin(\theta_k - \theta_M)}{h_{\text{eff}} \sin \theta_k} \right], \quad (6)$$

where $\chi_0 = M_s^2 / 3K$, $h_{\text{eff}} = h + \varepsilon m$, $h = H/H_k$, $m = M/M_s$. For $\varepsilon \neq 0$ this is an implicit equation which can be only solved by numerical methods. For a collection of randomly oriented easy axes, the RTS function can be obtained by integrating¹⁰ the above equation over θ_k and ϕ_k ; the texture distribution function (1) may also be introduced so as to model a realistic medium.⁸

If we consider the decay of the interacting magnetic system as described by Eq. (2), then its RTS should be modified in accordance with Eq. (5). In order to understand the resultant complex RTS curves we shall study some simple cases first.

Obviously, the RTS function approaches zero at strong applied fields \mathbf{H} and also if the magnetization is perpendicular to the applied field, that is, if it is parallel to the perturbing field \mathbf{h} . A thermally relaxing isolated particle yields, as shown in Fig. 4, RTS curves consisting of two branches associated with the two populations n_1 and n_2 on either side of the barrier. For inclination angles $\theta_k \geq 45^\circ$ the n_1 branch of RTS curves χ_t increases from zero at very strong fields (rightmost of Fig. 4) and then

smoothly drops off to zero again, passing through a maximum (Fig. 4). Although χ_t does not drop off to zero for angles $\theta_k < 45^\circ$ it still has a peak value at $H_n(\theta_k) < H < H_k$ for $\theta_k \geq \theta_c$. The critical inclination angle is numerically found to be $\theta_c \approx 32^\circ$. If $\theta_k < \theta_c$ then the peak of χ_t disappears and the RTS curves become monotonous (Fig. 4). The χ_t of n_1 branch always diverges at $-H_n$ for any angles of applied field. The same behavior of n_2 branch exists for the field sweeping reversely. In the hysteresis loop initially $n_1 \rightarrow 1$ and $n_2 \rightarrow 0$ and the n_1 branch dominates by virtue of Eq. (5). At $T=0$ the RTS switches branches only at $-H_n(\theta_k)$ where it diverges. However, due to thermal agitation this switching process takes place at smaller reversing fields.

The majority of switching events takes place at the critical field $-H_s > -H_n$ and the RTS curves switch from the n_1 to the n_2 branch. The exact behavior depends on the inclination angle θ_k : For a small θ_k there is a peak at coercivity, while at large θ_k one observes a dip $-H_c \geq -H_s$ (see Fig. 4). The divergence of χ_t at $-H_n(\theta_k)$ is removed for all inclination angles apart from the singular case of $\theta_k = 90^\circ$. The branches are exactly the same for either n_1 or n_2 at $\theta_k = 90^\circ$ regardless of thermal agitation, and thus the divergence of χ_t at anisotropy field always exists for any temperature at this singular angle.

Consider now the influence of coupling strength; For a randomly distributed system we find that with increasing

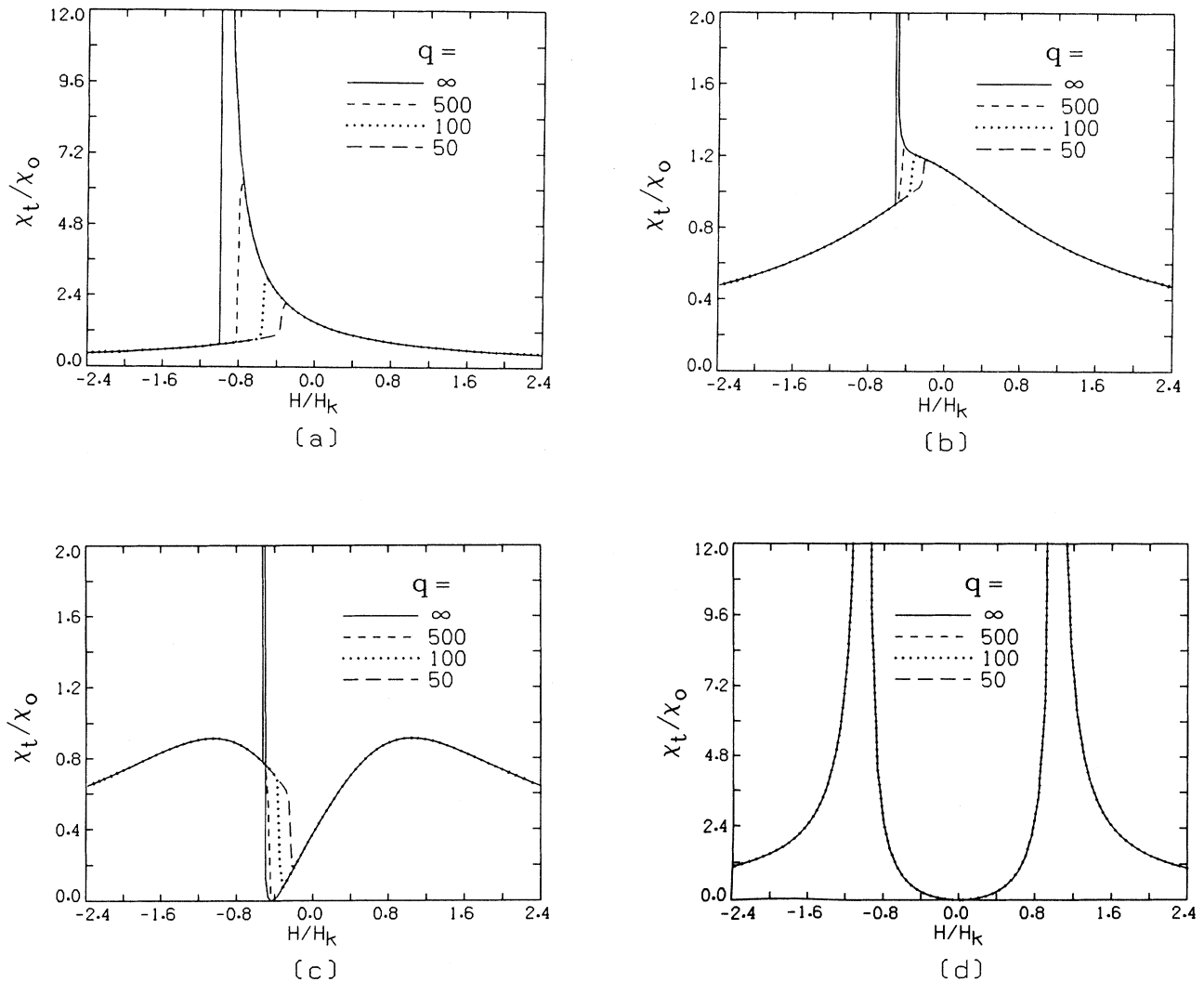


FIG. 4. The RTS functions of an isolated particle making an inclination angle θ_k of the easy axis with respect to \mathbf{H} . The right curve in the figures is the n_1 branch and the left curve is the n_2 branch. Branch switching takes place only at the nucleation field. Here $q = KV/k_B T$. (a) $\theta_k = 0^\circ$, (b) $\theta_k = 30^\circ$, (c) $\theta_k = 60^\circ$, (d) $\theta_k = 90^\circ$. Branch $n_1 \rightarrow n_2$ switches critically depends on temperature, however, at $\theta_k = 90^\circ$ the two branches are always the same and χ_t diverges at the anisotropy field H_k regardless of thermal agitation.

ε the peak in the RTS curves at the anisotropy field gradually merges with the peak at coercivity and then vanishes [Fig. 5(a)]; we shall show below that the shift varies linearly with coupling strength.¹⁰ It can, therefore, be concluded that the conventional peak detection method of RTS only yields the correct anisotropy field in a dilute system, while in a strongly interacting system it will either yield an incorrect anisotropy field or indicate its absence. A similar result has been observed in a barium ferrite system.⁶ It is worth mentioning that the peaks at $\pm H_k$ remain unaffected by temperature variations which suppress and shift the peak at coercivity [Fig. 5(b)]. The coercivity peak results from a sudden population change which is sensitive to all environmental factors. On the contrary, the anisotropy peak is mainly due to the presence of particles with large inclination angles (e.g., the divergence of χ_t at $\theta_k=90^\circ$) where the barrier height is almost the same from either direction and both minima are thus almost equally populated at any temperature.

It is known that real particulate media are usually oriented during the coating process so that the texture function (1) must be considered. To understand its influence in real media we should, in general, consider a distribution function of noncylindrical symmetry.⁸ It has been shown that in a noninteracting system the peak of

χ_t at H_c gradually decreases, while the peak at H_k become more pronounced, as the particles become better aligned⁸ and the number of particles with large θ_k increases. As discussed above, in an interacting system the anisotropy peak not only grows but also gradually merges with the coercivity peak as the coupling strength increases (Fig. 6). The coercivity peak thus becomes almost

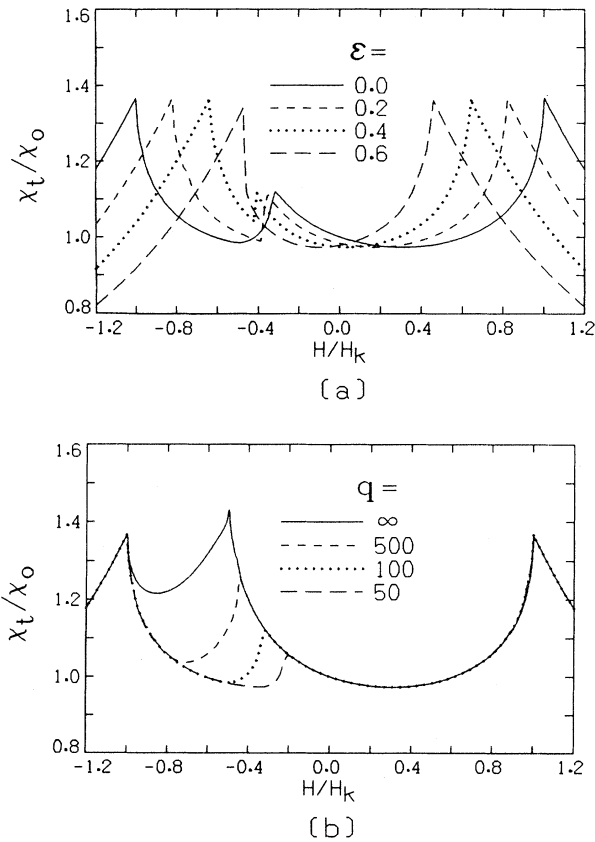


FIG. 5. The RTS functions of a randomly distributed system with different interparticle interaction (a) and at different temperatures (b). Here $f=0.1$ and $q=KV/k_B T$, (a) $q=100$; (b) $\varepsilon=0.0$.

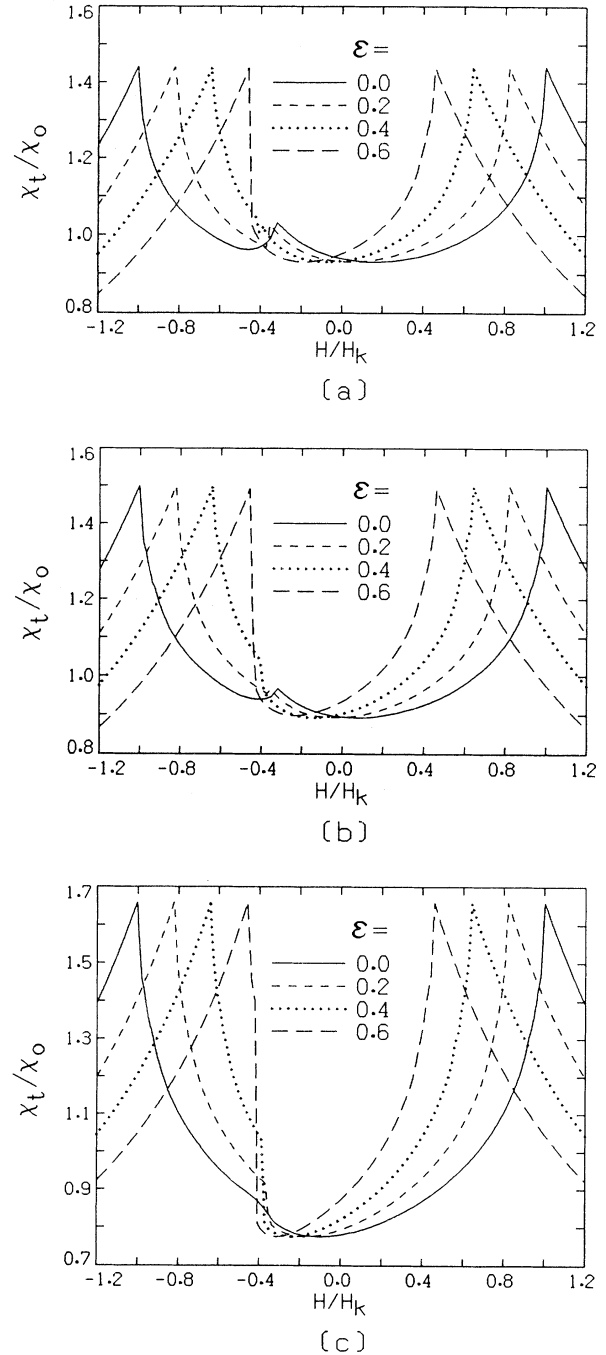


FIG. 6. The variation of χ_t versus the reduced field H/H_k for systems with varying texture and interaction strength ε ; $f=0.1$ and $KV/k_B T=100$. (a) $\sigma_\phi=2.0$ and $\sigma_\theta=2.0$; (b) $\sigma_\phi=1.5$ and $\sigma_\theta=1.5$; (c) $\sigma_\phi=1.0$ and $\sigma_\theta=1.0$.

unobservable in a well-aligned system while the anisotropy peak is enhanced till only one peak remains, located neither at $2K/M_s$ nor at coercivity (Fig. 6). The majority of particles in a well-aligned system have large θ_k and the RTS curve exhibits a dip (Figs. 4 and 6) rather than the peak encountered in randomly distributed systems. The peak detection techniques of coercivity in RTS curves thus fail in well-aligned systems, regardless of their coupling strength. It should be noted that RTS curves possibly show two peaks not only in a well-aligned (Fig. 6) but also in a strongly coupled system (Fig. 5). The coercivity peak disappears in a well-aligned system while the anisotropy peak merges with coercivity peak in a strongly coupled system. For a strongly coupled, well-aligned system, anisotropy peak shifts to the position of the dip at H_c [Fig. 6(c)].

The shift of the anisotropy peak towards the one at coercivity may easily be understood: Within the mean-field model particles experience the field $H + \alpha \langle M \rangle$. From previous studies of isolated particles, we know that the anisotropy peak mostly results from the $\theta_k = 90^\circ$ particles at $H_{\text{eff}} = H_k$ regardless of thermal agitation. Thus, for an interacting system, the anisotropy peak appears if the applied field $H = H_k - \alpha \langle M(H_k) \rangle \equiv H_k(\alpha)$. It fol-

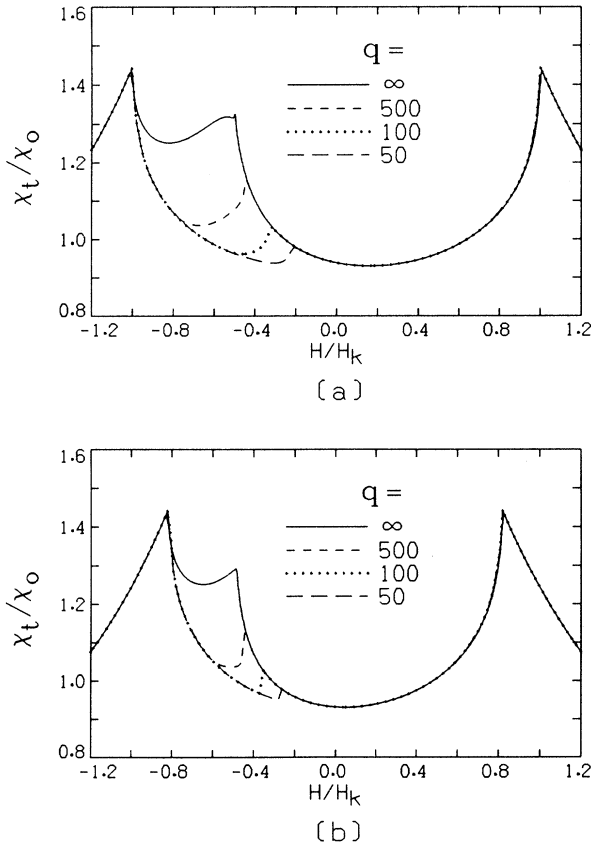


FIG. 7. The variation of χ_t versus the reduced field H/H_k for systems at different temperatures. Here $f=0.1$, and $q = KV/k_B T$. The texture parameters $\sigma_\theta = 2.0$ and $\sigma_\phi = 2.0$; (a) $\varepsilon = 0.0$; (b) $\varepsilon = 0.2$.

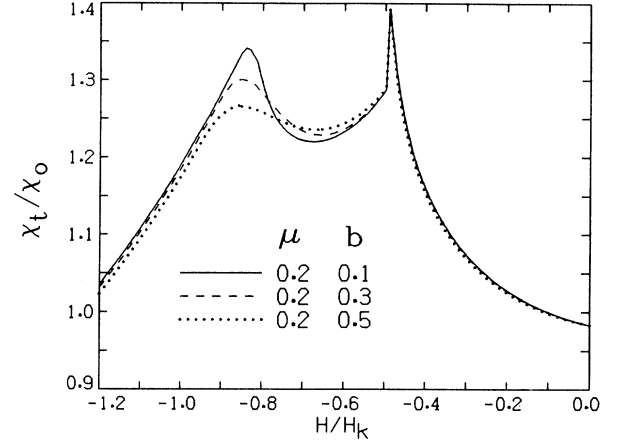


FIG. 8. χ_t for a random distribution of easy axes with several log-normal distributions of the coupling strength ε . The anisotropy peak is smeared out.

lows from here that the shift of the peak at $H_k(\varepsilon)$ is given by

$$H_k(\varepsilon) = H_k(1 - C\varepsilon), \quad \varepsilon \leq \varepsilon_{\text{max}}, \quad (7)$$

where $C = \langle M(H_k) \rangle / M_s$. The coercivity and anisotropy peaks merge at $\varepsilon = \varepsilon_{\text{max}}$ and from $H_k = H_c + \alpha_{\text{max}} \langle M(H_k) \rangle$ we finally obtain $\varepsilon_{\text{max}} = (M_s / H_k)(H_k - H_c) / \langle M(H_k) \rangle$. In general, H_c is a sensitive function of texture, temperature, and of the interaction strength, while $\langle M(H_k) \rangle$ is very insensitive to temperature changes, and so is the anisotropy peak of RTS. Indeed, increasing temperature shifts and suppresses the peaks at the coercivity but does not shift the anisotropy field peaks at all (Fig. 7). Both H_c and $\langle M(H_k) \rangle$ can be only determined numerically, e.g., $C = 0.913$ for a random distribution and $C = 1.0$ for perfect alignment; $\varepsilon_{\text{max}} = 0.575$ for a random distribution and $\varepsilon_{\text{max}} = 1.0$ for a perfectly aligned system without thermal agitation.

In a real material there is inevitably a distribution of interactions due to nonuniform particle packing. If we also consider a log-normal distribution of the interaction strength

$$P(\varepsilon) = \frac{1}{\sqrt{2\pi\varepsilon b}} \exp \left[-\frac{\ln^2(\varepsilon/\mu)}{2b^2} \right],$$

then the anisotropy peak becomes rounded and gradually smeared out but the coercivity peak remains about the same shape (Fig. 8). These rounded curves are consistent with the experimental data.^{4,6}

V. DISCUSSIONS AND CONCLUSIONS

The mean-field description of RS offers a method by which the simple model of coherent rotation can be extended to include interparticle interactions. The algorithm proposed here can approximately take into account hysteretic effects in interacting systems. The two-level system model employed here holds for positive coupling

strength only; for negative coupling the demagnetized antiferromagnetic state is favored at zero applied field and one needs at least one additional level to describe²⁵ the system dynamics.

We find that both texture and temperature can change the peak position at coercivity while the peaks at the anisotropy field maintain their position, though their shape is altered. We also find that a determination of the magnetic anisotropy field by means of the location of the peak in the transverse susceptibility curve can only be justified in a weakly interacting particle system. The anisotropy field of highly packed (strongly correlated) materials cannot be directly determined from the RTS data, however,

its value can be deduced from the linear expression of Eq. (7). In very strongly coupled systems all information about the anisotropy constant vanishes in RTS data.

Particular care must be taken in interpreting RTS data with only two peaks remaining: In a well-aligned system these peaks are associated with the anisotropy field but in a strongly coupled system they are associated with the coercivity.

ACKNOWLEDGMENT

This research has been partially supported by NSC Grant No. NSC-83-0208-M019-005, ROC.

-
- ¹P. M. Sallis, P. R. Bissell, P. I. Mayo, R. W. Chantrell, R. G. Gilson, and K. O'Grady, *J. Magn. Magn. Mater.* **120**, 94 (1993).
- ²W. Schmitt, *J. Magn. Magn. Mater.* **120**, 100 (1993).
- ³G. Asti and S. Rinalid, *J. Appl. Phys.* **45**, 3600 (1974).
- ⁴L. Pareti and G. Turilli, *J. Appl. Phys.* **61**, 5098 (1981).
- ⁵P. M. Sallis and P. R. Bissell, *J. Phys. D* **24**, 1891 (1991).
- ⁶H. J. Richter, *IEEE Trans. Magn.* **26**, 1882 (1990).
- ⁷A. Aharoni, E. M. Frei, S. Shtrikman, and D. Treves, *Bull. Res. Council. Isr. A* **6**, 215 (1957).
- ⁸A. Hoare, R. W. Chantrell, W. Schmitt, and A. Eiling, *J. Phys. D* **26**, 461 (1993).
- ⁹J. Lee, I. Klik, and Ching-Ray Chang, *J. Magn. Magn. Mater.* **129**, L141 (1994).
- ¹⁰Ching-Ray Chang and J.-S. Yang, *Appl. Phys. Lett.* **65**, 496 (1994).
- ¹¹J. J. Lu, H. L. Huang, Ching-Ray Chang, and I. Klik, *J. Appl. Phys.* **75**, 5499 (1994).
- ¹²A. Hoare, L. B. Uptonand, R. W. Chantrell, and Th. Orthand J. Pelzl (unpublished).
- ¹³Ching-Ray Chang and D. R. Fredkin, *IEEE Trans. Magn. MAG-22*, 391 (1986).
- ¹⁴J.-G. Zhu and H. N. Bertram, *J. Appl. Phys.* **63**, 3248 (1988).
- ¹⁵D. R. Fredkin and T. R. Koehler, *IEEE Trans. Magn. MAG-24*, 2371 (1988).
- ¹⁶D. C. Jiles and D. L. Atherton, *J. Magn. Magn. Mater.* **61**, 48 (1986).
- ¹⁷D. L. Atherton and R. Beattie, *IEEE Trans. Magn.* **26**, 3059 (1990).
- ¹⁸E. Callen, Y. J. Liu, and J. R. Cullen, *Phys. Rev. B* **16**, 263 (1977).
- ¹⁹D. K. Lottis, R. M. White, and E. Dan Dahlberg, *Phys. Rev. Lett.* **67**, 362 (1991).
- ²⁰E. C. Stoner and E. P. Wohlfarth, *Philos. Trans. Soc.* **240A**, 599 (1948).
- ²¹I. Klik, Ching-Ray Chang, and H. L. Huang, *Phys. Rev. B* **47**, 8605 (1993).
- ²²Ching-Ray Chang, *J. Appl. Phys.* **69**, 2431 (1991).
- ²³Hans-Benjamin Braun, *Phys. Rev. Lett.* **71**, 3557 (1993); J. J. Lu, H. L. Huang, and Ivo Klik, *J. Appl. Phys.* **76**, 1726 (1994).
- ²⁴Ching-Ray Chang and J. P. Shyu, *J. Appl. Phys.* **73**, 6659 (1993).
- ²⁵Ivo Klik, J.-S. Yang, and Ching-Ray Chang, *J. Appl. Phys.* **73**, 6493 (1994).
- ²⁶For negative interaction strength, the results are similar to the demagnetization field dominated relaxation of Ref. 19. Magnetization decays fast in the beginning and slower later on.
- ²⁷W. F. Jaep, *J. Appl. Phys.* **42**, 2790 (1971).